**RAA 2018** Vol. **18** No. **11**, 138(14pp) doi: 10.1088/1674–4527/18/11/138

*http://www.raa-journal.org* *http://iopscience.iop.org/raa*

***R**esearch in*
***A**stronomy and*
***A**strophysics*

# Improved semi-analytical computation of center manifolds near collinear libration points

Han-Qing Zhang and Shuang Li

College of Astronautics, Nanjing University of Aeronautics and Astronautics, Nanjing 210016, China
Advanced Space Technology Laboratory, Nanjing University of Aeronautics and Astronautics, Nanjing 210016, China; *lishuang@nuaa.edu.cn*

Received 2018 April 10; accepted 2018 May 29

**Abstract** In the framework of the circular restricted three-body problem, the center manifolds associated with collinear libration points contain all the bounded orbits moving around these points. Semi-analytical computation of the center manifolds and the associated canonical transformation are valuable tools for exploring the design space of libration point missions. This paper deals with the refinement of reduction to the center manifold procedure. In order to reduce the amount of calculation needed and avoid repetitive computation of the Poisson bracket, a modified method is presented. By using a polynomial optimization technique, the coordinate transformation is conducted more efficiently. In addition, an alternative way to do the canonical coordinate transformation is discussed, which complements the classical approach. Numerical simulation confirms that more accurate and efficient numerical exploration of the center manifold is made possible by using the refined method.

**Key words:** celestial mechanics — circular restricted three-body problem — center manifold — collinear libration point

## 1 INTRODUCTION

The study of dynamics near the collinear libration points in the Circular Restricted Three-Body Problem (CRTBP) has many practical applications in deep-space exploration missions. Due to the special dynamical and spatial properties they possess, regions around collinear libration points are suitable for setting up permanent observations of the Sun, the magnetosphere of the Earth, communication links with the far side of the Moon and so on. The linear character of the flow around the collinear libration points is of type center×center×saddle, which suggests that in addition to the stable and unstable manifolds, one can find another important type of manifold in the vicinity of collinear libration points, which is called the center manifold.

The center manifolds correspond to the center×center part of the dynamics near collinear libration points, which are also called neutrally stable manifolds (Gómez et al. 2001). Considering all the energy levels, the center manifolds are 4D in dimension. For a given energy level, they are 3D sets where dynamics have neutral behavior. Periodic and quasi-periodic orbits (invariant tori) can be found on the center manifolds. These manifolds play a crucial role in both astronomy and astrodynamics. The importance of center manifold computation can be summarized as follows:

(1) The center manifold is a global description of a neighborhood of collinear libration points, through which one can compute all kinds of periodic and quasi-periodic libration point orbits (LPOs) and gain understanding of how these orbits are organized.
(2) By canceling out the hyperbolic part, libration point dynamics can be reduced to the center manifold subspace, facilitating the study of long-term behavior of LPOs.
(3) In spatial CRTBP, the stable/unstable manifold of the center manifold (also known as the center stable/unstable manifold) is a 4D structure embedded

in a 5D energy surface in the phase space, which acts as a separatrix of qualitatively different motions, and provides additional opportunity and flexibility for transfer orbit design.

There are few papers dealing with computation of the collinear libration point center manifold. For Jacobi energy values close to one of the libration points, calculation of the center manifold can be conducted in a semi-analytical way. The calculation process consists of performing a reduction of the Hamiltonian that decreases the number of degrees of freedom, cancels out the hyperbolic component and allows numerical study of the Poincaré map near the collinear libration points (Gómez et al. 2001; Jorba & Masdemont 1999). This approach is known as reduction to the center manifold. This procedure can give a complete description of the libration orbits around an extended neighborhood of the collinear libration points. LPOs (such as planar and vertical families of Lyapunov periodic orbits, Lissajous orbits, periodic halo orbits and quasi-halo orbits) can be subsequently computed on the center manifold. Apart from the reduction to center manifold procedure, LPOs have also been computed through many approaches in the past. One common approach relies on Lindstedt–Poincaré methods to explicitly compute the periodic orbits and invariant tori (Gómez & Mondelo 2001; Richardson 1980). It tries to find approximate analytical expressions for LPOs in terms of appropriate amplitudes and phases.

Typical LPOs on the center manifold, such as halo, vertical and planar Lyapunov orbits, have already been studied in detail by Farquhar (1967); Farquhar & Kamel (1973); Hénon (1973); Henon (1997); Breakwell & Brown (1979); Howell (1984) and others. The analytical third-order expansions of collinear libration point halo orbits were first derived by Richardson (1980). Howell & Pernicka (1987) introduced a specialized two-layer numerical multiple-shooting method for the differential correction of approximate quasi-periodic LPOs. Barden (1998); Barden & Howell (1999) developed another method to compute quasi-periodic LPOs. After getting a linear approximation of a quasi-halo, they used it as an initial guess for a differential correction process, which patches a series of trajectory segments into a continuous orbit. Kolemen et al. (2012) presented another numerical method based on Fourier expansion for computing quasi-periodic orbits around collinear libration points. Ren & Shan (2014) recently introduced a fully numerical approach which can generate LPOs in the full solar system model without needing analytical approximations as initial guesses. Later, Zhang & Li (2016) proposed an LPO generation and extension method, with which structures like nested island chains and bounded chaotic motions have been revealed on the center manifold.

One disadvantage of most of these approaches is that they are not systematic LPO computation methods. Therefore, each LPO family (Lyapunov, halo, Lissajous, quasi-halo, etc.) must be dealt with separately. As a consequence, one LPO cannot be obtained before knowing its type. We implement an improved procedure for the computation of reduction to the center manifold in this paper, which can compute the LPOs in a unified and systematic way. In order to deal with the enormous polynomial computation involved in the process, we have proposed improved computation methods for the Hamiltonian of the center manifold and for the nonlinear canonical transformation, which can reduce the amount of calculations needed. Then an alternative way to do the canonical coordinate transformation is discussed. Finally, numerical explorations of the center manifold are carried out, which confirm that, with help from the refined method, a more accurate and efficient numerical exploration is made possible.

## 2 REDUCTION TO THE CENTER MANIFOLD PROCEDURE FOR THE CRTBP

In this section, we first recall the original procedure of reduction to the center manifold which is derived from the normal form computations (Gómez et al. 2001; Jorba & Masdemont 1999). The objective is removing some monomials in the expansion of the Hamiltonian of the CRTBP so as to obtain an invariant manifold tangent to the center directions. The key component of the procedure is performing a series of canonical changes of vari-

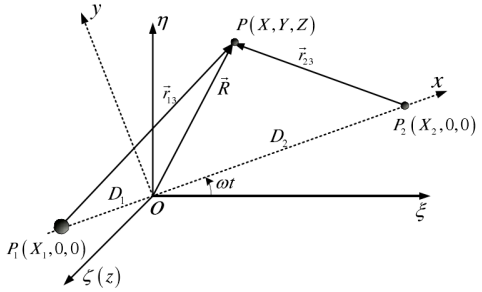


**Fig. 1** Geometry of the CRTBP.

ables, which can be implemented through means of the Lie series method (Deprit 1969).

In the framework of the CRTBP model, we assume two point masses, $P_1$ and $P_2$, are moving in circular orbits about their barycenter. The mass of the third body, $P$, is assumed to be infinitesimally small relative to the masses of $P_1$ and $P_2$. The parameter $\mu$ is the ratio of the mass of $P_2$ to the sum of masses of $P_1$ and $P_2$. The geometry of CRTBP is shown in Figure 1.

By normalizing the quantities and introducing a rotating synodic coordinate system with the barycenter located at the origin and two primaries fixed on the $x$-axis, a more convenient set of equations of motion can be derived, which is expressed in the form of the following series expansions (Jorba & Masdemont 1999)

$$\begin{cases} \ddot{x} - 2\dot{y} - (1+2c_2)x = \frac{\partial}{\partial x} \sum\limits_{n\geq 3} c_n(\mu)\rho^n P_n\left(\frac{x}{\rho}\right), \\ \ddot{y} + 2\dot{x} + (c_2-1)y = \frac{\partial}{\partial y} \sum\limits_{n\geq 3} c_n(\mu)\rho^n P_n\left(\frac{x}{\rho}\right), \\ \ddot{z} + c_2 z = \frac{\partial}{\partial z} \sum\limits_{n\geq 3} c_n(\mu)\rho^n P_n\left(\frac{x}{\rho}\right), \end{cases} \tag{1}$$

where $\rho^2 = x^2 + y^2 + z^2$, and $x$, $y$, $z$ are coordinates in the rotating CRTBP synodic coordinate system. The distance between the two primaries is normalized to 1. The left-hand side of Equation (1) contains the linear terms and the right-hand side has the nonlinear ones. $P_n$ are the Legendre polynomials. The coefficients $c_n(\mu)$ are given by

$$c_n(\mu) = \frac{1}{\gamma_j^3}\left((\pm 1)^n \mu + (-1)^n \frac{(1-\mu)\gamma_j^{n+1}}{(1\mp\gamma_j)^{n+1}}\right), \tag{2}$$

$$\text{for} \quad L_j, j = 1, 2,$$

$$c_n(\mu) = \frac{(-1)^n}{\gamma_3^3}\left(1 - \mu + \frac{\mu\gamma_3^{n+1}}{(1+\gamma_3)^{n+1}}\right), \tag{3}$$

$$\text{for} \quad L_3.$$

The Hamiltonian corresponding to Equation (1) takes the form

$$\begin{cases} H = H_2 - \sum\limits_{n>2} c_n(\mu)\rho^n P_n\left(\frac{x}{\rho}\right), \\ H_2 = \frac{1}{2}\Big(c_2\big(-2x^2 + y^2 + z^2\big) + 2yp_x - 2xp_y + p_x^2 + p_y^2 + p_z^2\Big). \end{cases} \tag{4}$$

Due to the linear character of the motion around collinear libration points being of type center×center×saddle, it is possible to transform the second order part of the Hamiltonian $H_2$ into its real normal form by using a symplectic real linear change of coordinates (Jorba & Masdemont 1999). For simplicity, the same name $H_2$ is used for the Hamiltonian:

$$H_2 = \lambda q_1 p_1 + \frac{\omega_p}{2}\left(q_2^2 + p_2^2\right) + \frac{\omega_v}{2}\left(q_3^2 + p_3^2\right), \tag{5}$$

where $\lambda$, $\omega_p$ and $\omega_v$ are real positive numbers. For the sake of simplifying the complexity of subsequent generating function computation, the second-order terms in $H_2$ were first diagonalized by introducing the following complex change of coordinates

$$\begin{cases} q_1 \to q_1, q_2 \to \frac{q_2 + ip_2}{\sqrt{2}}, q_3 \to \frac{q_3 + ip_3}{\sqrt{2}}, \\ p_1 \to p_1, p_2 \to \frac{p_2 + iq_2}{\sqrt{2}}, p_3 \to \frac{p_3 + iq_3}{\sqrt{2}}, \end{cases} \tag{6}$$

where the same variable names $q_1, q_2, q_3, p_1, p_2, p_3$ are used before and after the transformation for notational convenience. After changing the coordinates, $H_2$ in Equation (5) becomes

$$H_2 = \lambda q_1 p_1 + i\omega_p q_2 p_2 + i\omega_v q_3 p_3. \tag{7}$$

By applying this change of coordinates to the initial Hamiltonian $H$ in Equation (4), we can get

$$\begin{aligned} H(q,p) &= H_2(q,p) + \sum_{n\geqslant 3} H_n(q,p) \\ &= H_2(q,p) + \sum_{n\geqslant 3} h_{i_1,j_1,i_2,j_2,i_3,j_3} q_1^{i_1} p_1^{j_1} q_2^{i_2} p_2^{j_2} q_3^{i_3} p_3^{j_3} \ , \end{aligned} \tag{8}$$

where $H_2(q,p)$ is given by Equation (7) and $H_n(q,p)$ represents a degree $n$ homogeneous polynomial. From this point, the reduction to the center manifold process is similar to regular normal form computation. In order to transform Hamiltonian $H$ through the time one flow map of Hamiltonian $G$, we apply the Lie series canonical transformation formula

$$\hat{H} \equiv H + \{H,G\} + \frac{1}{2}\{\{H,G\},G\} + \frac{1}{3!}\{\{\{H,G\},G\},G\} + \cdots \ , \tag{9}$$

where $\hat{H}$ is the transformed Hamiltonian. Hamiltonian $G$ is the generating function of the transformation. The symbol $\{\cdot,\cdot\}$ denotes the Poisson bracket which can be defined for two smooth functions $F(q,p)$ and $G(q,p)$ as

$$\{F,G\} = \sum_{i=1}^{3} \left( \frac{\partial F}{\partial q_i}\frac{\partial G}{\partial p_i} - \frac{\partial F}{\partial p_i}\frac{\partial G}{\partial q_i} \right) . \tag{10}$$

Note that for the given homogeneous polynomials $P$ and $Q$ of degree $r$ and $s$ respectively, the Poisson bracket $\{P,Q\}$ is a homogeneous polynomial of degree $r+s-2$, which implies that for a generating function of degree 3, $G_3$, the transformed homogeneous polynomial of degree $n$, $\hat{H}_n$, is defined by

$$\begin{aligned} \hat{H}_2 &= H_2 \\ \hat{H}_3 &= H_3 + \{H_2, G_3\} \\ \hat{H}_4 &= H_4 + \{H_3, G_3\} + \{\{H_2, G_3\}, G_3\}/2 \\ &\vdots \end{aligned}$$

For the purpose of decoupling the hyperbolic direction from the center direction, some terms in the homogeneous polynomials $H_n$ should be eliminated. Assuming $H_n$ takes the form

$$H_n = \sum_{i_1+j_1+i_2+j_2+i_3+j_3=n} h_{i,j} q_1^{i_1} p_1^{j_1} q_2^{i_2} p_2^{j_2} q_3^{i_3} p_3^{j_3} \ , \tag{11}$$

and removing monomials in $H_n$ with $i_1 \neq j_1$, the generating function $G_3$ becomes

$$G_3(q,p) = \sum_{n=3} \frac{-h_{i_1,j_1,i_2,j_2,i_3,j_3}}{(j_1-i_1)\lambda + (j_2-i_2)i\omega_p + (j_3-i_3)i\omega_v} \times q_1^{i_1} p_1^{j_1} q_2^{i_2} p_2^{j_2} q_3^{i_3} p_3^{j_3} \ , \tag{12}$$

where $i_1 \neq j_1$. Applying $G_3$ to Equation (8), the Hamiltonian $\hat{H}$ takes the form

$$\hat{H}(q,p) = H_2(q,p) + \hat{H}_3(q,p) + \hat{H}_4(q,p) + \cdots \tag{13}$$

$$\hat{H}_3(q,p) = \hat{H}_3(q_1p_1, q_2, p_2, q_3, p_3) \ . \tag{14}$$

Similarly, this process can be applied recursively to find a homogeneous polynomial of degree four, $G_4$, and to eliminate monomials of order 4 from the new Hamiltonian, and so on for higher orders. In general, generating function of degree $n$, $G_n$, takes the form

$$\frac{-h_{i_1,j_1,i_2,j_2,i_3,j_3}}{(j_1-i_1)\lambda + (j_2-i_2)i\omega_p + (j_3-i_3)i\omega_v} \times q_1^{i_1} p_1^{j_1} q_2^{i_2} p_2^{j_2} q_3^{i_3} p_3^{j_3} \ , \tag{15}$$

where $i_1 \neq j_1$. Repeatedly applying this process to order $N$, the Hamiltonian finally gained has the form

$$\bar{H}(q,p) = H_2(q,p) + \bar{H}_2(q,p) + \cdots + \bar{H}_n(q,p) + R_N(q,p) = \bar{H}_N(q,p) + R_N(q,p) \ , \tag{16}$$

where

$$\bar{H}_N(q,p) \equiv \bar{H}_N(q_1p_1, q_2, p_2, q_3, p_3) \tag{17}$$

is a homogeneous polynomial of degree $N$ and $R_N$ is a remainder polynomial of order greater than $N$. Then, by neglecting the remainder polynomial and applying a canonical change given by $I = q_1p_1$, we obtain the Hamiltonian

$$\bar{H}_N(q,p) = H_2(I, q_2, p_2, q_3, p_3) + \sum_{n=3}^{N} \bar{H}_n(I, q_2, p_2, q_3, p_3) \ . \tag{18}$$

In order to cancel out the hyperbolic dynamics, we set $I = 0$. The Hamiltonian of the center manifold obtained this way is denoted as

$$H_N^{cm}(q_2, p_2, q_3, p_3) = \bar{H}_N(0, q_2, p_2, q_3, p_3) \ . \tag{19}$$

Finally, this center manifold Hamiltonian $H_N^{cm}$ is transformed back into its real form with the inverse transformation of Equation (6)

$$H_N^{cm}(q_2, p_2, q_3, p_3) = \frac{\omega_p}{2}\left(q_2^2 + p_2^2\right) + \frac{\omega_v}{2}\left(q_3^2 + p_3^2\right) + \sum_{n=3}^{N} H_n(q_2, p_2, q_3, p_3) \ . \tag{20}$$

According to the calculation process of center manifold Hamiltonian $H_N^{cm}$, the transformation process from CRTBP synodic coordinates to the center manifold coordinates can be represented as

$$\begin{aligned}(x, y, z, v_x, v_y, v_z) &\xleftarrow{A^{-1}} \left(x_1, y_1, z_1, p_{x1}, p_{y1}, p_{z1}\right) \xleftarrow{C^{-1}} \left(x_2, y_2, z_2, p_{x2}, p_{y2}, p_{z2}\right) \\ &\xleftarrow{D^{-1}} (q_1^2, p_1^2, q_2^2, p_2^2, q_3^2, p_3^2) \xleftarrow{G_3} (q_1^3, p_1^3, q_2^3, p_2^3, q_3^3, p_3^3) \\ &\xleftarrow{G_4} \cdots \xleftarrow{G_N} (q_1^N, p_1^N, q_2^N, p_2^N, q_3^N, p_3^N) \\ &\xleftarrow{D} (q_1^{cm}, p_1^{cm}, q_2^{cm}, p_2^{cm}, q_3^{cm}, p_3^{cm}) \ .\end{aligned}$$

Taking Earth-Moon $L_1$ point as an example, assuming $\gamma_1$ is the distance between $L_1$ and the Moon, the transformation $A$ corresponds to

$$\begin{cases} x \to x\gamma_1 - \gamma_1 - \mu + 1, y \to y\gamma_1, z \to z\gamma_1 \ , \\ v_{\mathrm{x}} \to p_{\mathrm{x}}\gamma_1 + y\gamma_1, v_{\mathrm{y}} \to p_{\mathrm{y}}\gamma_1 - x\gamma_1, v_z \to p_z\gamma_1 \ . \end{cases} \tag{21}$$

Transformation $C$ corresponds to the real linear canonical coordinate transformation:

$$(x, y, z, p_x, p_y, p_z)^{\mathrm{T}} = C \cdot (q_1, q_2, q_3, p_1, p_2, p_3)^{\mathrm{T}}$$

$$C = \begin{pmatrix} \frac{2\lambda}{s_1} & 0 & 0 & -\frac{2\lambda}{s_1} & \frac{2\omega_p}{s_2} & 0 \\ \frac{-2c_2+\lambda^2-1}{s_1} & \frac{-2c_2-\omega_p^2-1}{s_2} & 0 & \frac{-2c_2+\lambda^2-1}{s_1} & 0 & 0 \\ 0 & 0 & \frac{1}{\sqrt{\omega_v}} & 0 & 0 & 0 \\ \frac{2c_2+\lambda^2+1}{s_1} & \frac{2c_2-\omega_p^2+1}{s_2} & 0 & \frac{2c_2+\lambda^2+1}{s_1} & 0 & 0 \\ \frac{(1-2c_2)\lambda+\lambda^3}{s_1} & 0 & 0 & \frac{(2c_2-1)\lambda-\lambda^3}{s_1} & \frac{(1-2c_2)\omega_p-\omega_p^3}{s_2} & 0 \\ 0 & 0 & 0 & 0 & 0 & \sqrt{\omega_v} \end{pmatrix} . \tag{22}$$

$D$ corresponds to the transformation given in Equation (6). $D^{-1}$ represents the inverse transformation of $D$.

## 3 A REFINED HAMILTONIAN COMPUTATION METHOD FOR THE CENTER MANIFOLD

In order to illustrate the center manifold computation process, we take $N = 5$ as an example. Let $H$ denote the Hamiltonian before applying transformation $G_n$ and $\hat{H}$ signify the Hamiltonian after applying transformation $G_n$. Firstly, consider applying transformation $G_5$, according to Equation (9)

$$\hat{H}_2 = H_2, \quad \hat{H}_3 = H_3, \quad \hat{H}_4 = H_4, \quad \hat{H}_5 = H_5 + \{H_2, G_5\} \ , \tag{23}$$

therefore the Hamiltonian $H_2, H_3, H_4, H_5$ should be calculated first. Using transformation $G_4$, we can get

$$\hat{H}_2 = H_2, \quad \hat{H}_3 = H_3, \quad \hat{H}_4 = H_4 + \{H_2, G_4\}, \quad \hat{H}_5 = H_5 + \{H_3, G_4\} \ . \tag{24}$$

Continuing this backward derivation, with transformation $G_3$, we can get

$$\hat{H}_2 = H_2, \quad \hat{H}_3 = H_3 + \{H_2, G_3\}, \quad \hat{H}_4 = H_4 + \{H_3, G_3\} + \frac{1}{2}\{\{H_2, G_3\}, G_3\} \ , \tag{25}$$

$$\hat{H}_5 = H_5 + \{H_4, G_3\} + \frac{1}{2}\{\{H_3, G_3\}, G_3\} + \frac{1}{3!}\Big\{\{\{H_2, G_3\}, G_3\}, G_3\Big\} \ . \tag{26}$$

Following the above process, it can be found that before and after applying transformation $G_n$, $H_{n-1}, H_{n-2}, \cdots, H_2$ remain unchanged. In order to obtain the order $N$ center manifold, Hamiltonian $H_n, H_{n+1}, \cdots, H_N$ should be re-calculated when applying transformation $G_n$. For convenience of computer implementation, we can find that after applying transformation $G_m$, the Hamiltonian $H_n$ satisfies following equation

$$\begin{cases} \hat{H}_n = H_n + \Big\{H_{n-1}, G_m\Big\} + \dfrac{1}{2!}\Big\{\big\{H_{n-2}, G_m\big\}, G_m\Big\} + \cdots + \dfrac{1}{k!}\{\{\cdots\{H_{n-k}, G_m\}, G_m\}\cdots, G_m\} \ , \\ \qquad k \in \mathbb{N} \quad , \quad k < \dfrac{n-1}{m-2} \ . \end{cases} \tag{27}$$

It can be noticed that as the order $N$ of the center manifold increases, more and more Poisson bracket calculations are involved, and the number of terms in the homogeneous polynomial will increase exponentially. In order to reduce the amount of the calculation and improve efficiency, we re-examine Equations (23)–(26) and find that many Poisson brackets are computed more than once. Trying to avoid this kind of re-calculation, we check the interdependent relation between the Poisson brackets. Using transformation $G_3$ as an example, the Poisson brackets involved in the calculation of $\hat{H}_n$ are re-arranged into the following table form:

$$\begin{array}{lcccc} \hat{H}_3: & & & & H_2, G_3 \\ \hat{H}_4: & & & H_3, G_3 & H_2, G_3, G_3 \\ \hat{H}_5: & & H_4, G_3 & H_3, G_3, G_3 & H_2, G_3, G_3, G_3 \\ \hat{H}_6: & H_5, G_3 & H_4, G_3, G_3 & H_3, G_3, G_3, G_3 & H_2, G_3, G_3, G_3, G_3 \\ \vdots & & & \vdots & \end{array}$$

where the Poisson bracket $\{\{\cdots\{H_n, G_m\}, G_m\}\cdots, G_m\}$ is simply denoted as $H_n, G_m, \cdots, G_m$. It can be found that every column of Poisson brackets can be calculated recursively from top to bottom, and the calculation of each column is independent and thus parallelizable. Now check the transformation $G_4$:

$$\begin{array}{lccccc} \hat{H}_4: & & & & & H_2, G_4 \\ \hat{H}_5: & & & & H_3, G_4 & \\ \hat{H}_6: & & & H_4, G_4 & & H_2, G_4, G_4 \\ \hat{H}_7: & & H_5, G_4 & & H_3, G_4, G_4 & \\ \hat{H}_8: & H_6, G_4 & & H_4, G_4, G_4 & & H_2, G_4, G_4, G_4 \\ \vdots & & & \vdots & & \end{array}$$

Obviously, the recursive nature of each column has remained. The difference is that this table is interleaved with spaces. In general, we can summarize the refined calculation process for $\hat{H}_n, \hat{H}_{n+1}, \cdots, \hat{H}_N$ into the following steps:

(1) The total number of columns of Poisson brackets is $N - n + 1$. Counted from right to left, the column containing $H_2, G_n$ is denoted as column 1. Elements contained in column $i$ are denoted as $\mathrm{poisson}_1^i, \mathrm{poisson}_2^i, \cdots, \mathrm{poisson}_I^i$, where $I$ is

$$I = \left\lfloor \frac{-i - n + N - 1}{n - 2} + 1 \right\rfloor \ , \tag{28}$$

and $\lfloor \cdot \rfloor$ represents the operation of taking the integer part.

(2) Recursively calculate $\text{poisson}_1^i$, $\text{poisson}_2^i$, $\cdots \text{poisson}_I^i$ from top to bottom

$$\begin{cases} \text{poisson}_{k+1}^i = \left\{\text{poisson}_k^i, G_n\right\} \\ \text{poisson}_1^i = \{H_{i+1}, G_n\} \end{cases}, \qquad k = 1, 2, \cdots, I \ . \tag{29}$$

(3) According to Equation (27), assemble the calculated Poisson brackets into $\hat{H}_n, \hat{H}_{n+1}, \cdots, \hat{H}_N$

$$\hat{H}_{n-1+i} = H_{n-1+i} + \sum_{k=0}^{\lfloor \frac{i}{n-2} \rfloor} \frac{1}{(k+1)!} \text{poisson}_{k+1}^{i-k(n-2)}, \qquad i = 1, 2, \cdots, N-n+1 \ . \tag{30}$$

Note that in each column the elements are interleaved with $n-2$ spaces.

Applying this refined Hamiltonian computation method, the re-calculation of Poisson brackets can be completely avoided. Step (2) is the most computationally intensive process. As the calculation of each column is independent, it can be easily parallelized. Table 1 compares the computational efficiency of the original and the refined Hamiltonian computation methods. It can be seen that the refined method reduces the computation time dramatically.

## 4 REFINED METHODS FOR THE COMPUTATION OF CANONICAL COORDINATE TRANSFORMATION

Another crucial part of the reduction to the center manifold process is the computation of canonical transformation from center manifold coordinates to CRTBP synodic coordinates; in other words, an explicit expression for the change of variables that goes from the coordinates of the reduction to the center manifold to the CRTBP synodic coordinates. Based on this transformation, the periodic and quasi-periodic orbits can be computed systematically in synodic coordinates, as well as the Poincaré section of the center manifold in configuration space.

Once the generating function $G_3$ has been obtained, we can compute the corresponding transformation as

$$q_i^{(3)} = q_i + \{q_i, G_3\} + \frac{1}{2!}\{\{q_i, G_3\}, G_3\} + \frac{1}{3!}\{\{\{q_i, G_3\}, G_3\}, G_3\} + \cdots \ , \tag{31}$$

$$p_i^{(3)} = p_i + \{p_i, G_3\} + \frac{1}{2!}\{\{p_i, G_3\}, G_3\} + \frac{1}{3!}\{\{\{p_i, G_3\}, G_3\}, G_3\} + \cdots \ , \tag{32}$$

where $(q_1, p_1, q_2, p_2, q_3, p_3)$ denotes the coordinates after the transformation. In the next step, the generating function $G_4$ is applied to the right-hand side of the above equations, to obtain the change corresponding to fourth order, and so on continuing to higher orders

$$q_i^{(4)} = q_i^{(3)} + \left\{q_i^{(3)}, G_4\right\} + \frac{1}{2!}\left\{\left\{q_i^{(3)}, G_4\right\}, G_4\right\} + \frac{1}{3!}\left\{\left\{\left\{q_i^{(3)}, G_4\right\}, G_4\right\}, G_4\right\} + \cdots \ , \tag{33}$$

$$p_i^{(4)} = p_i^{(3)} + \left\{p_i^{(3)}, G_4\right\} + \frac{1}{2!}\left\{\left\{p_i^{(3)}, G_4\right\}, G_4\right\} + \frac{1}{3!}\left\{\left\{\left\{p_i^{(3)}, G_4\right\}, G_4\right\}, G_4\right\} + \cdots \ . \tag{34}$$

Finally, the nonlinear composite coordinate transformation of $G_3, G_4, \cdots, G_N$ takes the form

$$q_i^2 = q_i^{(N)}\left(q_1^N, p_1^N, q_2^N, p_2^N, q_3^N, p_3^N\right) \ , \tag{35}$$

$$p_i^2 = p_i^{(N)}\left(q_1^N, p_1^N, q_2^N, p_2^N, q_3^N, p_3^N\right) \ . \tag{36}$$

Because the Lie series calculation should be done on all six coordinates, the amount of computation for obtaining $q_i^{(N)}$ and $p_i^{(N)}$ is greater than for the center manifold computation itself. The methods from Section 3 can be adopted to dramatically reduce the computational effort. However, there is a difference: note that Equations (35) and (36) contain first order terms, which mean the corresponding Poisson brackets table has an additional row. Taking the $G_3$ transformation as an example, we have:

$$\begin{array}{lcccc}
\hat{H}_2: & & & & H_1, G_3 \\
\hat{H}_3: & & & H_2, G_3 & H_1, G_3, G_3 \\
\hat{H}_4: & & H_3, G_3 & H_2, G_3, G_3 & H_1, G_3, G_3, G_3 \\
\hat{H}_5: & H_4, G_3 & H_3, G_3, G_3 & H_2, G_3, G_3, G_3 & H_1, G_3, G_3, G_3, G_3 \\
\vdots & & & \vdots &
\end{array}$$

In practical applications, the transformation $q_i^{(N)}$ , $p_i^{(N)}$ usually needs to be applied to a large amount of coordinate points, in order to get a complete LPO in CRTBP synodic coordinates. Therefore, it is beneficial to speed up the application of $q_i^{(N)}$ and $p_i^{(N)}$ to numerical coordinates. Here we optimize the expression of $q_i^{(N)}$ and $p_i^{(N)}$ by introducing the Horner form of polynomials. Assuming the original polynomials have the form

$$P_n(x) = a_n x^n + a_{n-1}x^{n-1} + \cdots + a_0 \ , \tag{37}$$

and using a recursive algorithm, they can be re-organized into the following form

$$P_n(x) = ((a_n x + a_{n-1})x + \cdots)x + a_0 \ . \tag{38}$$

This is called the Horner form of polynomials (Knuth 1981). The Horner form uses less multiplication in the polynomial evaluation process, thus improving the computational efficiency. In order to illustrate the computation process, we take the 4th order Hamiltonian $H_4^{cm}$ of the Earth-Moon $L_1$ point center manifold as an example

$$\begin{aligned} H_4^{cm} = &- 0.0159p_2^4 - 0.0257p_2^3 - 0.0155p_3^2p_2^2 \\ &+ 0.289q_2^2p_2^2 + 0.216q_3^2p_2^2 + 1.17p_2^2 \\ &+ 0.496q_2^2p_2 + 0.428q_3^2p_2 + 0.033p_3q_2q_3p_2 \\ &- 0.141q_2^4 - 0.104q_3^4 + 1.13p_3^2 + 0.0994p_3^2q_2^2 \\ &+ 1.17q_2^2 + 0.0858p_3^2q_3^2 - 0.242q_2^2q_3^2 + 1.13q_3^2 \ . \end{aligned} \tag{39}$$

(1) Firstly, we take one of the variables which has the highest order in the expression. In this example, it is $q_3$. Then we treat $H_4^{cm}$ as a power series in $q_3$ and apply the Horner method

$$\begin{aligned} H_4^{cm} = &- 0.0159p_2^4 - 0.0257p_2^3 - 0.0155p_3^2p_2^2 \\ &+ 0.289q_2^2p_2^2 + 1.17p_2^2 + 0.496q_2^2p_2 \\ &- 0.141q_2^4 + 1.13p_3^2 + 0.0994p_3^2q_2^2 + 1.17q_2^2 \\ &+ q_3\left(0.03p_2p_3q_2 + q_3\left(0.21p_2^2 + 0.42p_2\right.\right. \\ &\left.\left.+0.085p_3^2 - 0.24q_2^2 - 0.1q_3^2 + 1.13\right)\right) \ . \end{aligned} \tag{40}$$

(2) Secondly, we take another variable which has the highest order in the expression. In this example, it is $q_2$. Then we treat the above equation as a power series in $q_2$ and apply the Horner method

$$\begin{aligned} H_4^{cm} = &- 0.0159p_2^4 - 0.0257p_2^3 - 0.0155p_3^2p_2^2 \\ &+ 1.17p_2^2 + 1.13p_3^2 + q_2^2\left(0.289p_2^2\right. \\ &\left.+0.496p_2 + 0.0994p_3^2 - 0.141q_2^2 + 1.17\right) \\ &+ q_3(0.03p_2p_3q_2 + q_3(0.21p_2^2 + 0.42p_2 \\ &+ 0.085p_3^2 - 0.24q_2^2 - 0.1q_3^2 + 1.13)) \ . \end{aligned} \tag{41}$$

(3) We repeat this process until the form of $H_4^{cm}$ no longer changes

$$\begin{aligned} H_4^{cm} = &p_2^2\left(-0.0155p_3^2 + \left(-0.0159p_2 - 0.0257\right)p_2\right. \\ &\left.+1.17\right) + 1.13p_3^2 + q_2^2\left(0.0994p_3^2 - 0.141q_2^2\right. \\ &\left.+ \left(0.289p_2 + 0.496\right)p_2 + 1.17\right) \\ &+ q_3\left(0.03p_2p_3q_2 + q_3\left(0.21p_2^2 + 0.42p_2\right.\right. \\ &\left.\left.+0.085p_3^2 - 0.24q_2^2 - 0.1q_3^2 + 1.13\right)\right) \ . \end{aligned} \tag{42}$$

After this optimization, the final form of $H_4^{cm}$ only needs 26 multiplications to be computed, instead of 57 multiplications in the original form. Generally speaking, the amount of calculation can be reduced by half with this

optimization. Nevertheless, repeated sub-expressions can still be found. With help from the Mathematica software system, this repeated calculation can be further eliminated by introducing intermediate variables

$$\begin{aligned} H_4^{cm} =&(0.033p_2p_3q_2 + ((0.216p_2 + 0.428)p_2 + 0.0858\text{temp}_1 - 0.242\text{temp}_3 \\ &- 0.104\text{temp}_4 + 1.13)q_3)q_3 + 1.13\text{temp}_1 \\ &+ ((-0.0159p_2 - 0.0257)p_2 - 0.0155\text{temp}_1 + 1.17)\text{temp}_2 \\ &+ ((0.289p_2 + 0.496)p_2 + 0.0994\text{temp}_1 - 0.141\text{temp}_3 + 1.17)\text{temp}_3 \ , \end{aligned} \tag{43}$$

where $\text{temp}_1 = p_3^2, \text{temp}_2 = p_2^2, \text{temp}_3 = q_2^2$ and $\text{temp}_4 = q_3^2$. These two kinds of optimization can usually speed up the application of coordinate transformation by a factor of 2 to 3.

## 5 THE SECOND KIND OF THE COORDINATE TRANSFORMATION METHOD

As a complement to the method introduced in Section 4, here we propose the second kind of coordinate transformation method. The theoretical basis of this method is the same as the former method, but as opposed to the transformation sequence $G_3 \to G_4 \to \cdots \to G_N$ used in Section 4, we first consider the generating function $G_N$ and write the transformation in vector function form

$$\bar{X} = \Phi_N(X) = \begin{cases} p_i + \{p_i, G_N\} + \dfrac{1}{2!}\{\{p_i, G_N\}, G_N\} + \cdots, & i = 1, 2, 3 \\ q_i + \{q_i, G_N\} + \dfrac{1}{2!}\left\{\left\{q_i^2, G_N\right\}, G_N\right\} + \cdots, & i = 1, 2, 3 \end{cases} \tag{44}$$

where $X = (q_1, p_1, q_2, p_2, q_3, p_3)$ denotes the coordinates before the transformation, $\bar{X} = (\bar{q}_1, \bar{p}_1, \bar{q}_2, \bar{p}_2, \bar{q}_3, \bar{p}_3)$ denotes the coordinates after the transformation and $\Phi_N$ denotes the transformation from $X$ to $\bar{X}$. Similarly, we can obtain transformation functions $\Phi_{N-1}, \Phi_{N-2}, \cdots, \Phi_3$ corresponding to $G_{n-1}, G_{n-2}, \cdots, G_3$, respectively. Note that in all of these calculations, $q_i$ or $p_i$ represents the variable itself, not the complicated expression of the former calculation. Then the complete nonlinear transformation function can be written as the composition of $\Phi_{N-1}, \Phi_{N-2}, \cdots, \Phi_3$

$$\hat{X} = \Phi_{N,N-1,\cdots,3}(X) = \Phi_3\Big(\cdots\left(\Phi_{N-1}\left(\Phi_N(X)\right)\right)\Big) \ . \tag{45}$$

Note that it is impractical to evaluate this expression for symbolic $X$ coordinates. However, this expression can be evaluated efficiently when a set of numerical values of $X$ is given.

The distinguishing feature of this transformation method is that it breaks the whole nonlinear transformation process into smaller ones. Each transformation function $\Phi_n$ has a relatively simple expression. When implemented on a computer, this method can avoid simultaneously loading very big expressions into the memory, thus it is more memory-efficient, lowering the hardware requirements. The expression of $\Phi_3, \Phi_4, \cdots, \Phi_N$ can be further optimized with the Horner form and common sub-expression extraction method.

Table 2 compares the two coordinate transformation methods by means of the expression generating time and the expression application time. It is clear that the first kind of transformation method needs more time to generate the enormous transformation expression. The generated expression needs to be held in a large amount of computer memory. However, once the transformation expression has been generated, application of the transformation to specific numerical coordinates is fast. On the other hand, the second kind of transformation method needs little time to generate the transformation expression $\Phi_3, \Phi_4, \cdots, \Phi_N$, but application of the transformation to specific numerical coordinates is slower, which suggests that it is suitable for conditions when the computer memory is limited or the transformation is not applied very often.

## 6 NUMERICAL RESULTS

With help from the refined computation method, the center manifold has been computed up to order 17, making accurate and efficient numerical exploration possible. Combining the refined Hamiltonian computation method and the coordinate transformation method, we can systematically compute all kinds of periodic and quasi-

**Table 1** Computation time comparison between the original and refined Hamiltonian computation methods (time unit: second, program running on AMD Phenom II 940 CPU ).

| Computation order | Original method | Refined method (single thread) | Refined method (four parallel threads) |
|---|---|---|---|
| $N = 4$ | 0.078 | 0.016 | 0.006 |
| $N = 5$ | 0.094 | 0.046 | 0.017 |
| $N = 6$ | 0.422 | 0.171 | 0.059 |
| $N = 7$ | 0.827 | 0.499 | 0.166 |
| $N = 8$ | 2.715 | 1.466 | 0.489 |
| $N = 9$ | 5.507 | 3.947 | 1.317 |
| $N = 10$ | 15.818 | 9.189 | 3.516 |

**Table 2** Comparisons of the two coordinate transformation methods by means of the expression generating time and the expression application time.

| Computation order | The first kind of method | | The second kind of method | |
|---|---|---|---|---|
| | Generation time (s) | Application time (s) | Generation time (s) | Application time (s) |
| $N = 8$ | 7.581 | 0.016 | 3.666 | 0.019 |
| $N = 10$ | 46.036 | 0.031 | 16.021 | 0.047 |
| $N = 12$ | 197.232 | 0.047 | 41.715 | 0.109 |

periodic orbits on the center manifold and subsequently transform them back to the CRTBP synodic coordinates. After the Hamiltonian $H_N^{cm}$ of the center manifold is computed, the equation of motion in center manifold coordinates can be derived

$$\begin{cases} \dot{q}_2 = \dfrac{\partial H_N^{cm}}{\partial p_2}\,, \quad \dot{q}_3 = \dfrac{\partial H_N^{cm}}{\partial p_3}, \\ \dot{p}_2 = -\dfrac{\partial H_N^{cm}}{\partial q_2}, \quad \dot{p}_3 = -\dfrac{\partial H_N^{cm}}{\partial q_3}, \end{cases} \tag{46}$$

The system admits one conservative quantity given by $H_N^{cm}$

$$H_N^{cm}(q_2, p_2, q_3, p_3) = C_{\text{center}}\ . \tag{47}$$

The following numerical computations presented here are done in the Earth–Moon CRTBP with mass parameter $\mu = 0.01215$. The non-dimensional units of distance, velocity and time are denoted by DU, VU and TU respectively, where 1 DU = 384 400 km, 1 VU$= 1.0183\,\mathrm{km\,s^{-1}}$ and 1 TU = 377490.606 s.

The refined center manifold computation method has been implemented on a homogeneous cluster with 64 2.8 GHz AMD 6380 kernels. The numerical integration of the CRTBP trajectory has been carried out with a high accuracy Bulirsch-Stoer extrapolation method (Press 2007). Figures 7 and 8 show two typical examples of LPOs computed with this process.

In order to understand the whole structure of the center manifold, we try to reduce the degrees of freedom by only looking at orbits on the center manifold in the same energy level, thus only three free variables remain. A further reduction of degrees of freedom can be obtained by looking at the orbits where they cross a surface of section (also known as a Poincaré section). Through this procedure, all the libration orbits with a fixed Hamiltonian value $C_{\text{center}}$ can be obtained by tuning two variables with regard to the initial conditions.

Figure 2 shows the $L_1$ center manifold structure on the Poincaré section $p_2 = 0$ for energy level $C_{\text{center}} = 0.7$.

It is clear that the Poincaré map on the Poincaré section $p_2 = 0$ is symmetric with respect to both the $q_3$ axis and the $p_3$ axis. A fixed point is located at the origin $(q_3 = 0, p_3 = 0)$, corresponding to the planer Lyapunov orbit. It can be found that the planer Lyapunov orbit has an asymptotic orbit associated with it, which suggests that the planer Lyapunov orbit is hyperbolically unstable on the center manifold. The asymptotic orbit also acts as the separatrix between different kinds of motion, in this

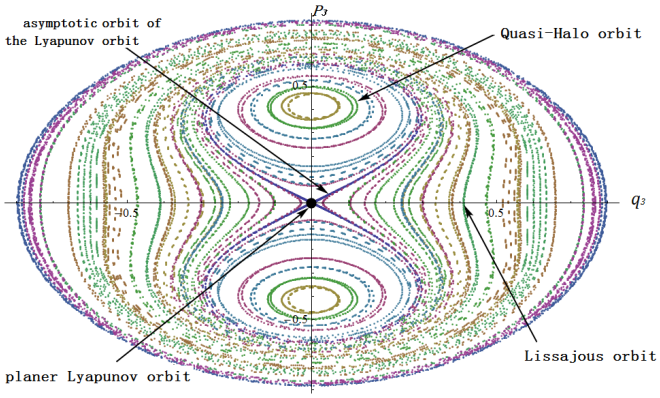


**Fig. 2** $L_1$ center manifold structure on the Poincaré section $p_2 = 0$ for energy level $C_{\text{center}} = 0.7$.

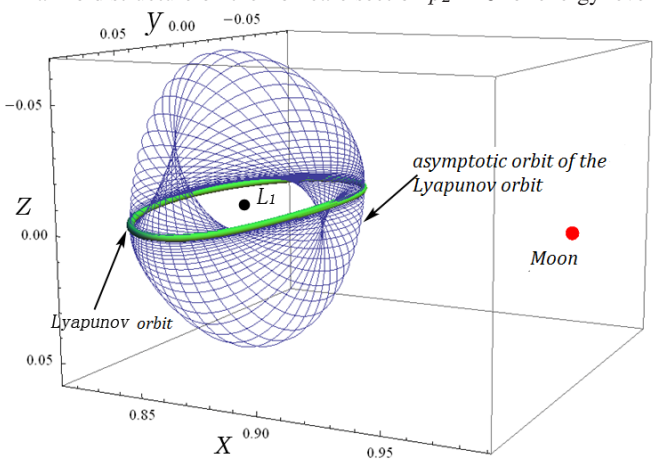


**Fig. 3** The asymptotic orbit of the Lyapunov orbit in CRTBP configuration space.

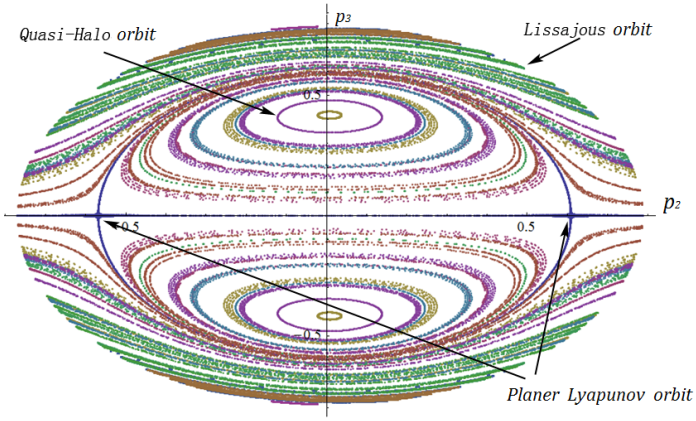


**Fig. 4** $L_1$ center manifold structure on the Poincaré section $q_3 = 0$ for energy level $C_{\text{center}} = 0.7$.

case separating Lissajous orbits from quasi-halo orbits. Figure 3 shows the asymptotic orbit computed in CRTBP configuration space. This type of orbit can be utilized in a future mission design process to transfer a spacecraft from a planar periodic LPO to an inclined orbit without $\Delta v$ cost.

Alternatively, the Poincaré section can be chosen to be $q_3 = 0, p_3 = 0$, possibly revealing other aspects of

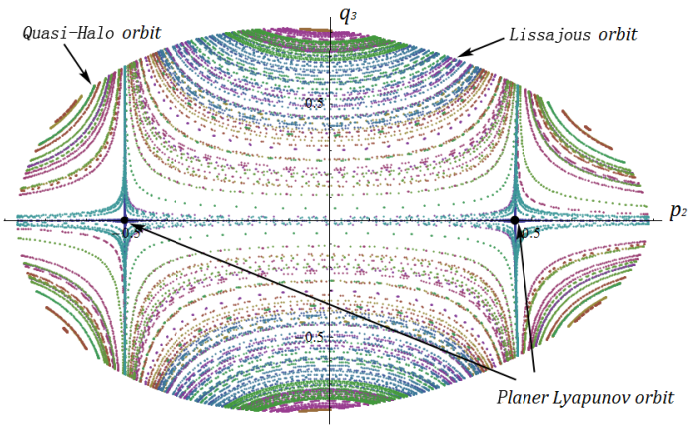


**Fig. 5** $L_1$ center manifold structure on the Poincaré section $p_3 = 0$ for energy level $C_{\text{center}} = 0.7$.

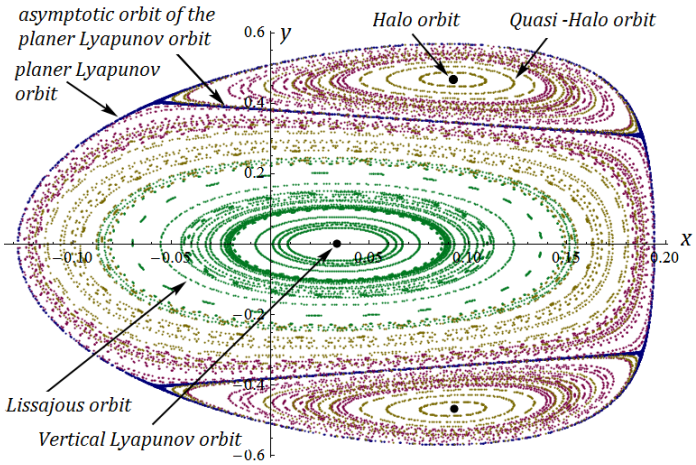


**Fig. 6** $L_1$ center manifold structure on the Poincaré section $z = 0$ in CRTBP synodic coordinates with energy level $C_{\text{center}} = 0.7$.

the structure of the center manifold. The $L_1$ center manifold structures on these Poincaré sections are shown in Figures 4 and 5. It can be found that the asymptotic orbit still acts as the separatrix between qualitatively different kinds of motion. On the Poincaré section $q_3 = 0$, while the section of quasi-halo orbits remains as closed curves, the section of Lissajous orbits does not. In comparison, on the Poincaré section $p_3 = 0$, the sections of quasi-halo orbits and Lissajous orbits both become segmented curves.

Finally, by utilizing the refined coordinate transformation method, we can efficiently compute Poincaré maps of the orbits constituting the center manifold in CRTBP synodic coordinates for a given energy level; one example with $C_{\text{center}} = 0.7$ is shown in Figure 6. The results are very similar to the results obtained by Gómez & Mondelo (2001). Due to the underlying $x$-$z$ plane symmetry of the CRTBP equation, structures on this Poincaré section show symmetry about the $x$-axis. The boundary encompassing the whole region is the planar Lyapunov orbit. It is the only periodic orbit on the center manifold that lies completely in the $x$-$y$ plane. The region inside the planar Lyapunov orbit is divided into three parts by the curve corresponding to the asymptotic orbit of the planar Lyapunov orbit. The central part consists of a series of concentric invariant curves corresponding to Lissajous type quasi-periodic orbits. The upper and lower parts of the region consist of another set of concentric invariant curves corresponding to quasi-halo orbits. These curves surround the fixed points that correspond to the well-known halo orbits. Because the motion in the center manifold is represented uniformly in Equation (46), all these types of LPOs can be generated in a unified manner with the refined methods by choosing suitable initial conditions.

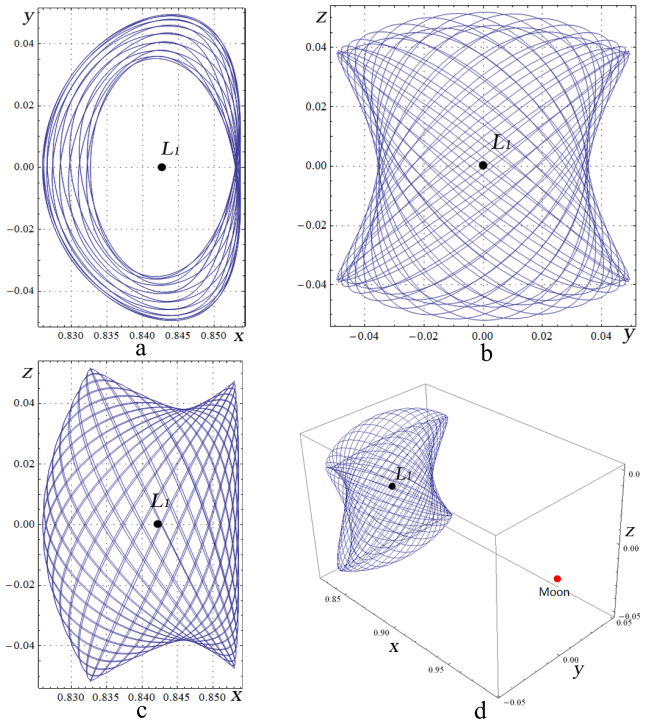


**Fig. 7** Lissajous orbit in CRTBP synodic coordinates, computed with the refined Hamiltonian computation method and coordinate transformation method (a: $x$-$y$ plane projection, b: $z$-$y$ plane projection, c: $x$-$z$ plane projection, d: 3D projection).

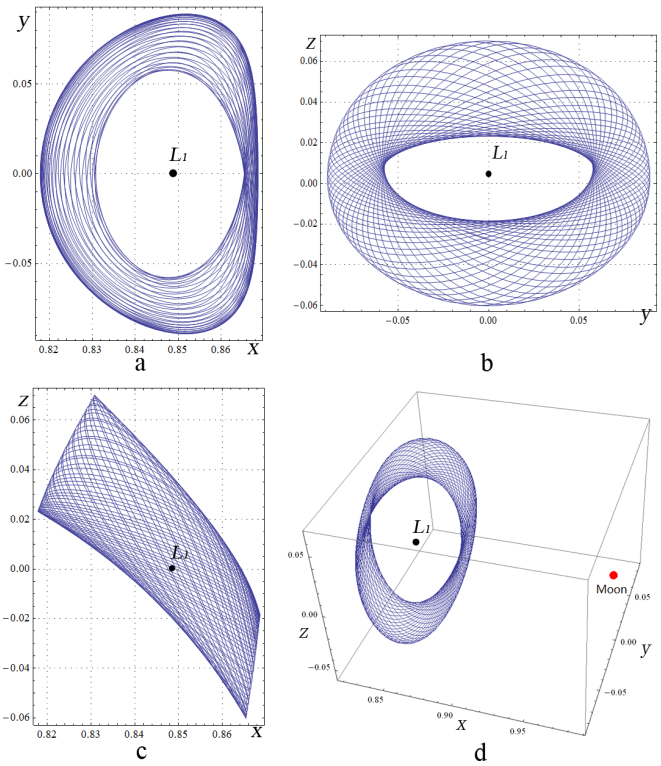


**Fig. 8** Quasi-halo orbit in CRTBP synodic coordinates, computed with the refined Hamiltonian computation method and coordinate transformation method (a: $x$-$y$ plane projection, b: $z$-$y$ plane projection, c: $x$-$z$ plane projection, d: 3D projection).

## 7 SUMMARY AND REMARKS

In the process of reduction to the center manifold, the amount of polynomial computation grows exponentially with the order of the center manifold. In order to reduce the amount of calculation, avoiding repetitive computation of Poisson bracket, an improved method is presented, which is inherently parallelizable. By using the Horner form and the method of extracting common subexpressions, an optimized form of the polynomial expression is obtained. Finally, a new way to do the canonical coordinate transformation is discussed. Through the refined methods introduced here, the center manifold computation can be carried out to higher orders, facilitating more accurate and efficient libration point mission design processes.

**Acknowledgements** This work was supported by the National Natural Science Foundation of China (Grant Nos. 11403013 and 11672126), the Fundamental Research Funds for the Central Universities (Nos. 56XAA14093 and 56YAH12036) and the Postdoctoral Foundation of Jiangsu Province (No. 1301029B).

### References

Barden, B. T. 1998, in Proceedings of the AAS/AIAA Space Flight Mechanics Meeting, Monterey, 1998, 969

Barden, B. T., & Howell, K. C. 1999, Astrodynamics, 2000, 2307

Breakwell, J. V., & Brown, J. V. 1979, Celestial Mechanics, 20, 389

Deprit, A. 1969, Celestial Mechanics, 1, 12

Farquhar, R. W. 1967, Journal of Spacecraft and Rockets, 4, 1383

Farquhar, R. W., & Kamel, A. A. 1973, Celestial Mechanics, 7, 458

Gómez, G., Jorba, A., Simó, C., & Masdemont, J. 2001, Dynamics and Mission Design Near Libration Points: Volume III: Advanced Methods for Collinear Points (World Scientific)

Gómez, G., & Mondelo, J. M. 2001, Physica D Nonlinear Phenomena, 157, 283

Hénon, M. 1973, Celestial Mechanics, 8, 269

Henon, M. 1997, Generating Families in the Restricted Three-Body Problem (Berlin: Springer-Verlag)

Howell, K. C. 1984, Celestial Mechanics, 32, 53

Howell, K. C., & Pernicka, H. J. 1987, Celestial Mechanics, 41, 107

Jorba, À., & Masdemont, J. 1999, Physica D Nonlinear Phenomena, 132, 189

Knuth, D. E. 1981, The Art of Computer Programming. 2: Seminumerical Algorithms (Reading, Mass.: Addison-Wesley, 1981, 2nd ed.)

Kolemen, E., Kasdin, N. J., & Gurfil, P. 2012, Celestial Mechanics and Dynamical Astronomy, 112, 47

Press, W. H. 2007, Numerical Recipes 3rd edition: The Art of Scientific Computing (Cambridge: Cambridge University Press)

Ren, Y., & Shan, J. 2014, Celestial Mechanics and Dynamical Astronomy, 120, 57

Richardson, D. L. 1980, Celestial Mechanics, 22, 241

Zhang, H., & Li, S. 2016, Celestial Mechanics and Dynamical Astronomy, 126, 339